International Journal of Adhesion & Adhesives 134 (2024) 103787

Contents lists available at ScienceDirect

International Journal of Adhesion and Adhesives

journal homepage: www.elsevier.com/locate/ijadhadh

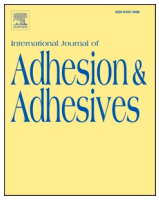

Analysis of creep crack growth in bonded joints based on a Paris' law-like approach

E. Meulman [a], J. Renart [a,c,*], L. Carreras [a], J. Zurbitu [b]

[a] AMADE, Polytechnic School, University of Girona, Campus Montilivi, s/n, 17071, Girona, Spain
[b] Ikerlan Technology Research Centre, Basque Research and Technology Alliance (BRTA), Arrasate-Mondragón, Spain
[c] Serra Húnter Fellow, Generalitat de Catalunya, Spain

ARTICLE INFO

Keywords:
Creep crack growth
Bonded joint
FEM
TDCB
Wedge test

ABSTRACT

Creep crack growth is one of the factors that could affect the durability of a bonded joint and compromise the safety of structures over long periods of time. However, numerical tools and test methods relating to creep crack growth in bonded joints are not widely available yet. In this work, a Creep Crack Growth Model (CCGM) is proposed for adhesively bonded joints. The model describes the relation between the crack growth rate and the energy release rate. The CCGM is fitted with results from Roller Wedge Driven creep crack growth (RWDC) tests and validated against the results obtained from tapered double cantilever beam (TDCB) tests with a constant load applied. Additionally, it is demonstrated that the proposed model can be introduced in a fatigue tool commercially available from the finite element method (FEM) code Abaqus to predict creep crack growth. The FEM results show that the phenomenological expression fitted from experimental tests results, which is used as input for the FEM tool, is reproduced with accuracy. Moreover, it is shown that the CCGM is capable of predicting creep crack growth rates when a different specimen geometry is used, thus demonstrating that the model correctly captures the physics of the problem.

Nomenclature

a	Crack length
B	Width of specimen
c	Empirical parameter for the creep crack growth model
C	Compliance
da/dt	Crack growth rate
dC/da	Compliance rate related to the crack length
G	Energy release rate
G_c	Fracture toughness
h	Thickness of the adherend
m	Specimen geometry factor
P	Applied load
s	Empirical parameter for the creep crack growth model describing the slope
t_a	Bondline thickness
BK	Benzeggagh and Kenane fracture criterion
CBT	Corrected Beam Theory
CCGM	Creep Crack Growth Model
CZM	Cohesive Zone Model
DC	Direct Cyclic
DCB	Double Cantilever Beam
ECM	Experimental Compliance Method
FE	Finite Element
FEM	Finite Element Method
LVDT	Linear Variable Displacement Transducer
RWD	Roller Wedge Driven
RWDC	RWD creep crack growth
TDCB	Tapered Double Cantilever Beam
VCCT	Virtual Crack Closure Technique

(*continued on next column*)

(*continued*)

1. Introduction

The durability of bonded joints is essential for ensuring the safe and reliable operation of structures over long periods of time. One of the factors which can reduce the strength and longevity of the bonded joint is creep crack growth, which could be considered as time dependent. The creep crack growth process involves slow, time-dependent deformation of the adhesive material under a constant stress caused by the existence of a defect in the adhesive in the form of a sharp crack tip. Looking at the bonded joint from a macroscopic perspective, creep

* Corresponding author. AMADE, Polytechnic School, University of Girona, Campus Montilivi, s/n, 17071, Girona, Spain.
E-mail addresses: edwin.meulman@udg.edu (E. Meulman), jordi.renart@udg.edu (J. Renart), laura.carreras@udg.edu (L. Carreras), jzurbitu@ikerlan.es (J. Zurbitu).

https://doi.org/10.1016/j.ijadhadh.2024.103787
Received 12 July 2024; Accepted 15 July 2024
Available online 16 July 2024

deformation occurs within a defined area known as the Fracture Process Zone (FPZ), delineated by the point where the adhesive joint cannot endure any further traction (stress-free region), and the point where the adhesive joint begins to degrade.

Creep crack growth resistance of bonded joints is influenced by the type of material and adhesion with the adherends, the geometry of the joint, and the environmental conditions. Selecting the appropriate adhesive can help to improve the durability of the joint [1–5].

The damage tolerance approach relies on the remaining capacity of a structure to safely sustain in-service loads, even when sub-critical sized cracks are present. Applying this approach to adhesively bonded joints, crack growth is allowed as long as it does not reach an unsafe size during service. To determine the time needed for this occurrence, employing microstructural models to assess creep deformation of the adhesive ahead of the crack tip is not practical. Conversely, Linear Elastic Fracture Mechanics (LEFM) methodologies offer a viable approach to predict the load causing creep crack propagation, relying on a singular metric—the energy release rate (ERR). Within LEFM, the fracture toughness (G_c) is considered a material property providing a macroscopic understanding of fracture propagation. Thus, to predict the time required for an existing crack to reach an unsafe size it is useful to establish the relationship between the crack growth rate (da/dt) and the severity of the loading conditions, i. e. the energy release rate (ERR).

Many widely used engineering tools for structural design and international standards determining fracture properties are based on LEFM concepts. However, methods relating to time dependent crack growth in bonded joints are not widely available yet. Some researchers have tried to use existing methods like, for example, the Boeing wedge test [6] (standard withdrawn in 2019) that was originally designed for qualitative testing but using it to obtain quantitative data [7,8]. The standard only compares crack length and fracture surface between specimens. In this test, the wedge remains stationary inside the specimen, resulting in a change of the stress state at the crack tip when the crack propagates [9]. The question arises how fast the energy release rate changes when a stationary wedge is used, preventing the stabilization of the fracture process zone, and thus leading to a different crack growth rate than the one observed in a constant energy release test.

Different test setup configurations have been developed to test with a constant energy release rate. Plausinis et al. [9] and Dillard et al. [10] make use of a cable system with weights and Lefebvre et al. [11] and Nakamura et al. [12] use springs trying to keep the energy release rate constant with crack extension. All these examples make use of double cantilever beam (DCB) specimens, and the test is load controlled by using weights or springs. Although, when a DCB specimen is loaded under load control, the distance between the load point and the crack tip increases during crack propagation, and the energy release rate is not constant over time. Schrader et al. [13] has tried to solve that by using a computer-controlled system that constantly calculates the energy release rate with the J-integral method and corrects the load applied by the test machine. This requires sophisticated test equipment which is not widely available. Meulman et al. [14,15] have tried to simplify the test setup configuration by making use of a moving roller wedge that is loaded with a small constant weight, so there is no need of a test machine or large complex test setup. The advantage of a moving wedge is that the distance between the wedge and crack tip remains constant during the crack propagation phase [14,16,17]. Another option could be to change the type of specimen and use for instance a tapered double cantilever beam (TDCB) specimen instead of a more commonly used DCB specimen [18]. The main advantage of the TDCB is that the compliance rate with respect to the crack length remains constant due to the tapered section of the adherends [19]. This means that during crack propagation, if the load remains constant, the energy release rate also does [18]. TDCB specimens used for mode I tests on adhesively bonded joints can be found in literature [20–26]. However, as far as the authors know, it has not been used for time dependent crack growth tests by applying a constant load to the TDCB specimen by use of weights. A certain known weight can be hung at the bottom adherend, using the same connecting pin system as would be used for a quasi-static TDCB test in a tensile test machine. Over time, the crack will propagate due to the constant energy release rate introduced by the constant load.

In this work, creep crack growth curves are obtained by measuring crack propagation over time in constant load TDCB tests. Moreover, these curves are used in a finite element (FE) model to predict creep crack growth in an adhesively bonded joint. As far as the authors know, a commercially available FEM module to simulate time dependent crack growth in a bonded joint is not available yet. In this case, the authors adapted the Direct Cyclic (DC) module for fatigue crack growth available from the FEM software Abaqus [27] for creep crack growth prediction. VCCT is used to calculate the energy release rate. Examples of models that make use of the DC module for fatigue simulation in Abaqus are Pirondi et al., Dávila et al. and Teimouri et al. [28–30]. The DC module requires the input of a Paris' law-like expression to simulate the crack growth rate related to a certain energy release rate. The required input Paris' law-based curves are obtained from experimental results where the crack growth rate per cycle (da/dN) is plotted against the energy release rate on a log-log scale. Here, the fatigue crack growth rate per cycle (da/dN) is replaced by the crack growth rate per unit of time (da/dt).The authors demonstrate that using the VCCT in combination with the DC module could be used to simulate time dependent crack growth in bonded joints. The relationship between the different experimental tests and the numerical model of this work is presented in a visual flowchart in Fig. 1 and described in more detail in Section 2, 3 and 4. First a Creep Crack Growth Model (CCGM) is introduced (Fig. 1, step 1) and fitted with the results from the RWDC tests obtained in previous work (Fig. 1, step 2) [14]. Then, a 2D numerical model of the TDCB specimen is created and the CCGM is introduced in the FE model (Fig. 1, step 3). Test results from the TDCB constant load test are presented and compared with the RWDC results (Fig. 1, step 4 & 5). Finally, the FE results are compared to the experimental test results (Fig. 1, step 6).

2. Methodology

In this section, the Creep Crack Growth Model (CCGM) is presented. Secondly, the roller wedge driven creep crack growth (RWDC) test method proposed in Ref. [14] is described. Experimental results of the adhesive in study are used to adjust the CCGM parameters. Instructions for implementing the CCGM in the DC method available in Abaqus FE code are given.

2.1. Creep crack growth model

The CCGM is based on the hypothesis that the crack growth rate (da/dt) is controlled by the energy release rate (G). In the proposed model a Paris' law-like power law describes this relationship:

$$da/dt = c \cdot \left(\frac{G}{G_c}\right)^s \tag{1}$$

where da/dt is the crack growth rate against the time, G the energy release rate, c and s are empirical material parameters. The energy release rate is normalized with the fracture toughness (G_c) obtained from quasi-static tests. The idea is that, if CCGM is plotted on a log-log scale, it forms a log-linear trendline, similar as the that obtained from experimental fatigue results. The crack growth has to be measured under constant G conditions, which corresponds to a stationary regime, where the generation of a Fracture Process Zone (FPZ) in the adhesive is set, and which is not taken into account in the analysis. Experimental tests must be performed at different levels of G to find parameters c and s so that the model describes the creep crack growth curve for that specific bonded joint.

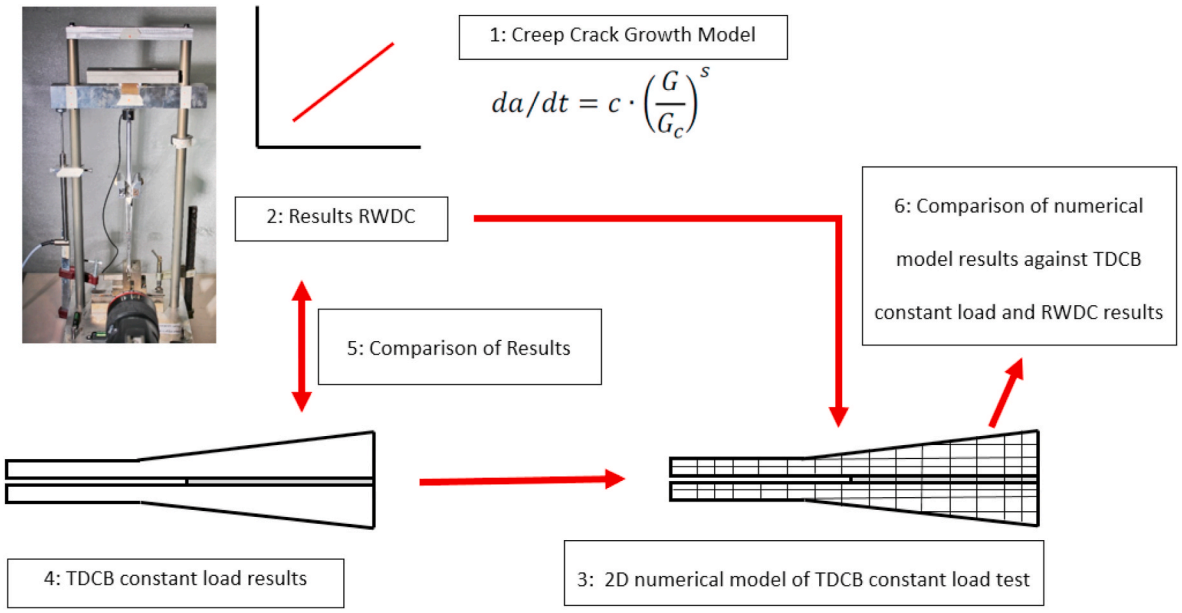

Fig. 1. Flowchart of the methodology, validation and results comparison.

2.2. RWD creep crack growth test method (RWDC)

The RWDC test method makes use of a roller wedge [14] to apply a constant energy release rate in mode I. The roller wedge consists out of three small rollers of 6 mm in diameter (Fig. 2, right). The roller wedge is inserted in a pre-cracked DCB-like specimen which is clamped in vertical position (Fig. 2, left). On top of the roller wedge, a weight is placed so that during the creep crack growth test the energy release rate is constant regardless of the crack length. During crack propagation, the roller wedge follows the crack tip, so that the displacement of the wedge

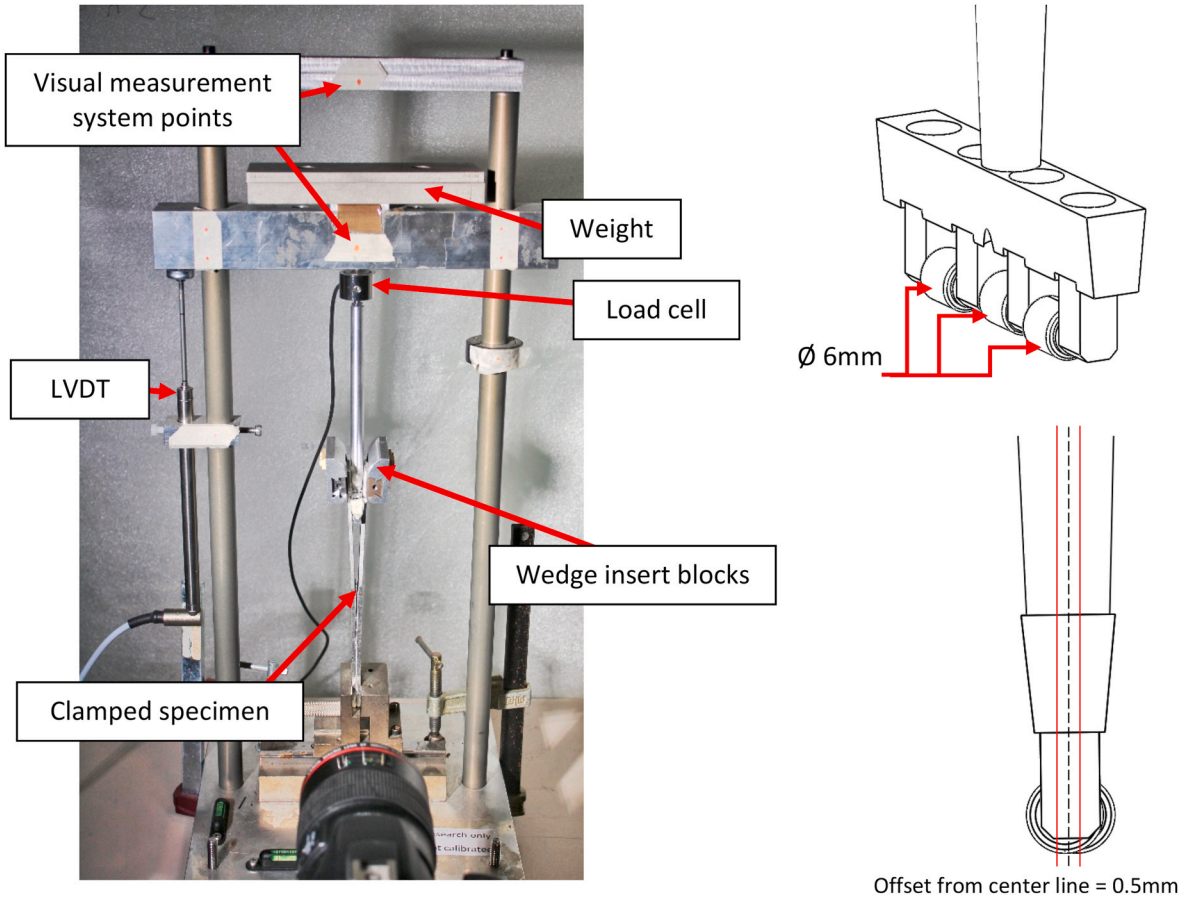

Fig. 2. Left: Test setup of the RWDC test method. The specimen is vertically clamped and loaded with a weight on top of the wedge. Right: Schematic drawing of roller wedge [14].

equals the crack length increase. With a Linear Variable Displacement Transducer (LVDT) the displacement of the roller wedge is measured over time. The RWD data reduction method [14] is used to calculate the energy release rate:

$$G = \frac{3}{4}\frac{E_x h^3 \delta_y^2}{\left(\sqrt[4]{\frac{3}{4}\frac{E_x B h^3 r_w^2}{F_{Push|s}}} + \chi h\right)^4} \quad (2)$$

where h is the thickness of the adherend, B the width of the specimen, E_x is the longitudinal Young's modulus of the adherend, δ_y is the opening displacement at the contact point between the roller and the adherend, r_w is the radius of the wedge tip (roller radius), χ is the crack length correction factor [31], and $F_{Push|s}$ is measured with the load cell and is the force that is applied to the wedge. Rollers are used to reduce the friction to a minimum so in the data reduction method the friction coefficient can be assumed zero, and, therefore, friction is neglected in the data reduction method. The bondline thickness is indirectly considered in the parameter δ_y in equation (2), which is described in more detail in the RWD test methodology presented in previous work [15].

In a previous test campaign [14] crack growth rates vs constant energy release rate were obtained and are presented in Fig. 3. The specimens tested were DCB-like aluminium specimens bonded with Araldite 2021-1. Every data point represents one tested specimen. Plotting the constant applied energy release rate against the measured crack growth rate on a log-log scale gives a log-linear trendline that can be described with the CCGM (equation (1)), where c = 4.13 and s = 3.90. The test results from Fig. 3 are used to validate the CCGM with the TDCB constant load tests. Also, the results are used to demonstrate that the CCGM can be implemented in an existing commercially available numerical model.

2.3. Introduction of the CCGM into a commercial fatigue crack growth tool

A 2D finite element model of a tapered double cantilever beam (TDCB) specimen is created in Abaqus/CAE (6.14-2) [27] to demonstrate that a commercially available fatigue tool that is based on a Paris' law-like expression can be used to simulate creep crack growth based on the proposed model. The TDCB adherends are modelled with CPE4I 4-node bilinear plane strain elements with incompatible modes. The size of the elements is 0.5 mm × 0.5 mm. The bondline is modelled as a surface-to-surface contact, assuming zero thickness. The VCCT is applied to the row of nodes connecting the two adherends, which then represents the adhesive, to evaluate the energy release rate. A Griffith criterion is used to release the nodes when the energy release rate equals the mode I fracture toughness of the adhesive, propagating the crack to the next pair of nodes. This means that the crack propagates with increments of 0.5 mm (element length). The B–K mode-interpolation for the critical energy release rate is used with the same value for all three modes (G_{Ic}) obtained from TDCB quasi-static experimental tests.

The DC model is used to simulate crack propagation over a certain time period. However, this module requires a frequency as input relating to the number of cycles that is applied in fatigue. Taking a frequency of 1 Hz automatically results in $da/dN = da/dt$ (dt in seconds). In that way, da/dt obtained from the creep crack growth test results can be directly implemented in the Paris' law-like equation of the DC module. The material parameters from the RWDC results (Fig. 3, c = 4.13 and s = 3.90) are entered in the DC module. Fig. 4 shows the cycle that the DC module in Abaqus requires to simulate the creep crack growth in a bonded joint. As the tool was designed for simulating fatigue crack growth, the crack will not propagate in the DC module unless it is subjected to an amplitude. The amplitude of 1 (Fig. 4) relates to the constant load (nodal point load in y-direction) applied to one of the adherends. At

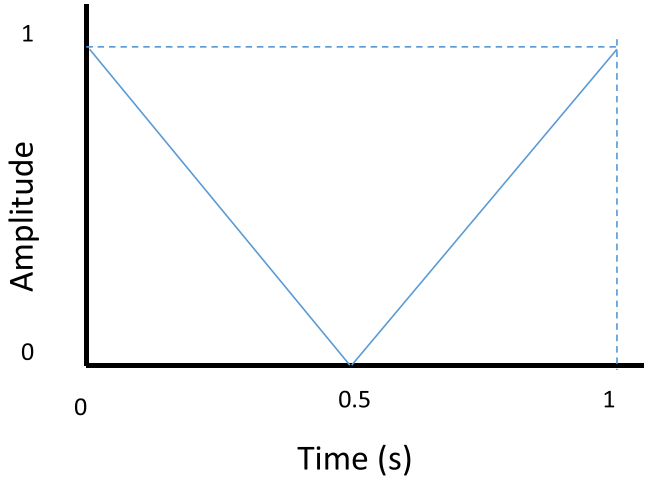

Fig. 4. Required input cycle in the DC module of Abaqus to simulate creep crack growth in a bonded joint.

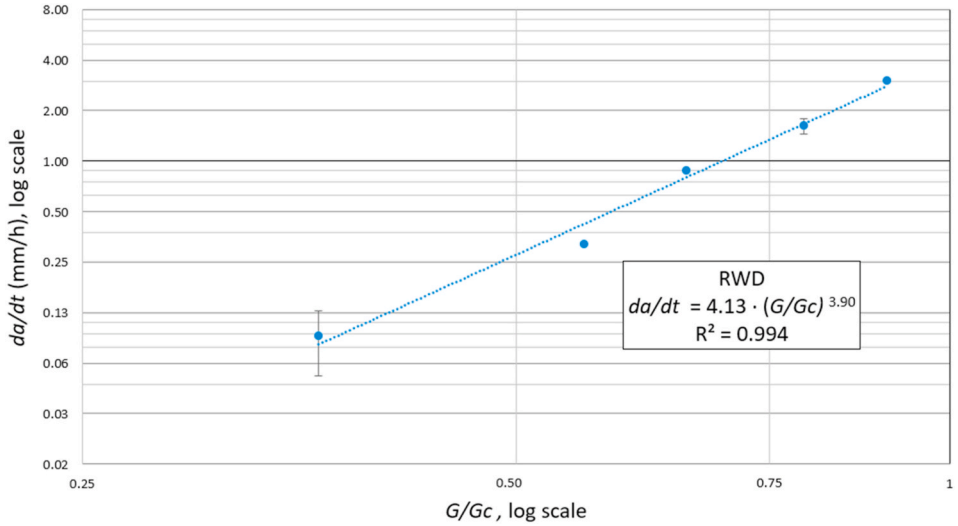

Fig. 3. Creep crack growth curve obtained with the RWDC test method in previous work [14].

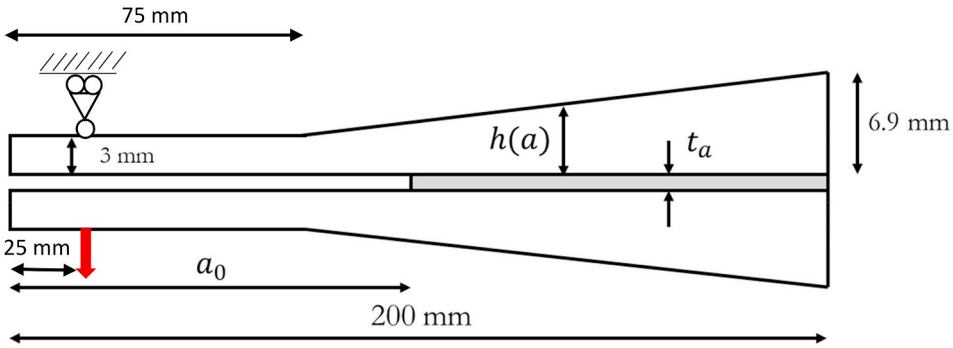

Fig. 5. TDCB specimen design with a width of 25 mm and a tapered geometry factor m of 278 mm^{-1}.

this loading point (arrow in Fig. 5) the adherend is only constrained in x-direction. The other adherend is constrained in both x and y-direction at a single node symmetric to the loading point (Fig. 5), so that the specimen can open freely. The VCCT computes the envelope energy release rate at the start and end of each cycle, which will drive the crack propagation following the entered CCGM parameters in the Paris' law-like equation of the DC module. 25 Fourier terms and a time point every 0.25 s was selected based on a trade-off between accuracy and computational efficiency. Running the FEM model for various constant loads will result in different energy release rates.

Fig. 5 shows the TDCB specimen geometry design created in the FEM model.

This specimen design is chosen to maintain a constant compliance rate during crack propagation, the adherend thickness (h) has to be chosen in such a way that the specimen geometry factor m remains constant while a is increasing [18]:

$$m = \frac{3a^2}{h^3} + \frac{1}{h} \tag{3}$$

where h is the adherend thickness and a the crack length.

The adherends are made from aluminium Al 7075-T6 with a width of 25 mm and a Young's modulus of 71 GPa, shear modulus of 27 GPa and a yield strength of 550 MPa and the dimensions described in Fig. 5. The adherends are modelled with isotropic elastic behaviour. Besides the tapered section, the rest of the specimen dimensions (width and thickness of the aluminium substrates), as well as the adhesive layer properties are the same as the DCB-like specimens used for the RWDC tests in previous work [14].

3. Validation of the creep crack growth model

To validate the creep crack growth model TDCB specimens are manufactured and tested by applying a constant load. The specimens are also tested in a quasi-static manner to have a reference value for the fracture toughness for this specific bonded joint. In this section the experimental method for testing the TDCB specimen quasi-static and with a constant load is described.

The TDCB specimens were tested and manufactured at the AMADE research group testing laboratory at the University of Girona (ISO17025 and NADCAP certified). The temperature and relative humidity in the laboratory are $(23 \pm 2)^{\circ}C$ and (50 ± 5) %RH, respectively. Specimens were in-house manufactured by bonding aluminium Al 7075-T6 adherends with Araldite 2021-1. Before bonding, the adherends received a surface treatment with a sandblaster using brown fused aluminium oxide of 60 μm. After sandblasting, the adherends were cleaned using acetone and just before applying the adhesive the adherends were decreased with high grade alcohol. Teflon spacers were used to create the bondline thickness. To enhance the curing process the specimens were placed in a 60 °C oven for 16 h. The dimensions of the specimens obtained are specified in Fig. 5.

The TDCB quasi-static test is outlined in ISO standard 25217:2009 [18]. The widely employed DCB test for bonded joints is likewise described in this ISO standard due to their close similarity in test principles, with the only difference being the geometry. For the TDCB the experimental compliance method (ECM) reads:

$$G_{Ic} = \frac{P^2}{2B}\frac{dC}{da} \tag{4}$$

with P being the applied load, B the width of the specimen, C the compliance (specimen opening displacement divided by the load) and a the crack length. As mentioned before, a TDCB specimen is designed to maintain a constant value for dC/da during crack propagation. This value follows directly from the slope obtained by plotting the linear fit of experimental results of compliance against the crack length. The crack length was measured by using a traveling camera and marks on the side of the specimen. The specimen was loaded by an MTS insight 5 kN tensile test machine with a constant displacement rate of 2 mm/min.

A test frame was designed to be able to test two TDCB constant load tests in parallel (Fig. 6). The specimens are first pre-cracked under quasi static conditions for about 15 mm in the MTS insight 5 kN tensile test machine. The same loading blocks and pins are used to connect the specimens to the test frame as used for the quasi-static test. At the bottom, a weight hung from the specimen that opens as the crack propagates. Two canon cameras with a macro lens are used to take photos at 12 h interval to capture the crack propagation over time.

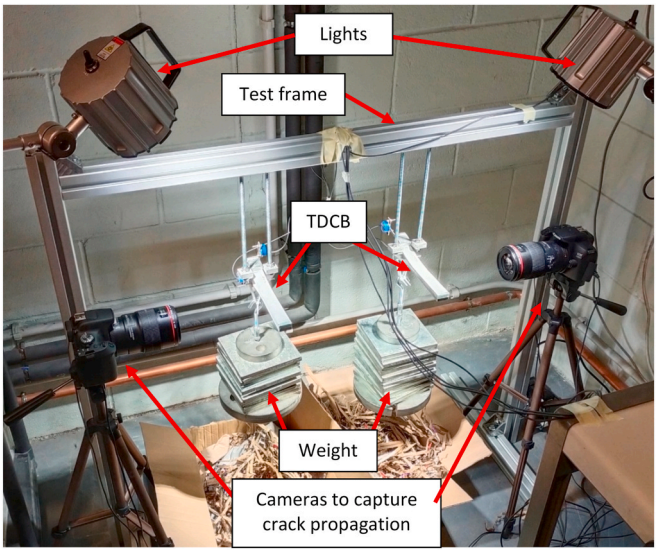

Fig. 6. TDCB constant load test frame and canon cameras to capture the crack propagation over time. The two cardboard boxes below the weights are just there to provide a soft landing for the weights when the specimens fail.

The specimens' long sides are painted white and marks are applied in the same way as was done for the quasi-static TDCB test. ImageJ software is used to manually measure the crack length in the photos. The marks are used to calibrate the visual measurement. Fig. 7 shows an example of a painted and marked TDCB specimen, where the dashed line arrow indicates the calibration of the pixel measurement in the photo. The solid line arrow indicates how the crack length is determined measured from the tip of the pre-crack. The dark lines beneath the red arrow result from shadows cast by overhead lighting. These shadows emerge due to slight irregularities on the adhesive surface along the specimen's sides.

A total of seven TDCB specimens were tested. Table 1 shows an overview of the specimens tested with the number of specimens per type of test method.

Performing tests at different load levels has been prioritized against repeating the same test conditions at the same load level. The alignment of the data points on the same curve suggests low dispersion within the dataset.

4. Results

Results of the TDCB quasi-static test, constant load test and FEM model are presented in this section. First, the fracture toughness is obtained from three TDCB specimens tested under quasi-static conditions. With the TDCB constant load test, the creep crack growth rates are obtained for different applied loads and plotted on a log-log scale to obtain the creep crack growth curves. Finally, FEM results are presented and compared against the RWDC method and the TDCB constant load test.

4.1. TDCB quasi-static test

The results of the quasi-static tests are shown in Fig. 8 where the energy release rate is plotted against the crack length. It can be observed that the energy release rate for every individual specimen stays relatively constant during crack propagation. However, there is spread between the three specimens. Note that TDCB_01 lacks crack length data for the initial phase because no clear crack propagation can be observed in the photos. Considering the data beyond 100 mm of crack propagation, the values range from 2 to 3 kJ/m^2.

The specimens are opened completely after the quasi-static tests to inspect the fracture surfaces. All three specimens show cohesive failure. Specimen TDCB_01 is shown in Fig. 9 as an example of the cohesive fracture surface observed. This type of fracture surface was also found in previous work for DCB and RWD test with the same adhesive Araldite 2021–1 [15].

Table 2 shows data of the three specimens with, B the width of the specimen, dC/da which is the slope found when the compliance is plotted against the crack length, and the fracture toughness determined with the ECM data reduction method (equation (4)) [18].

Table 1
Tested specimens overview.

Specimen	Test method	Disp. rate (mm/min)	t_a (mm)	No. of specimens
TDCB_0x	TDCB quasi-static	2	0.89 ± 0.05	3
TDCB_CL_0x	TDCB constant load	–	0.79 ± 0.09	4

4.2. TDCB constant load test

Based on results of the quasi-static TDCB tests, different loads are selected to be applied to the specimens for the TDCB constant load tests. The load applied to each specimen is presented in Table 3. The constant energy release rate applied to the specimen is calculated by using the ECM data reduction method (equation (4)). The design of the TDCB determines dC/da (Table 2) and is constant during crack propagation, specimen width B can be found for each specimen in Table 3.

In Fig. 10, the crack length is plotted against the time for TDCB_CL_01. The curves can be divided in two parts with different slopes: the initial part shows already crack growth but at a relatively low rate compared to the second part. This initial part, which happens already inside the tapered section, is considered as the onset slope. The second part of the curve starts after about 75 h, and it is the propagation slope. For this specific test, the propagation slope ends at around 180 h because the crack approaches the end of the specimen and results in sudden complete rupture of the specimen. It was demonstrated in previous work that this particular adhesive system shows a transitory phase before the steady-state crack propagation phase [14]. This initial transitory phase precedes the establishment of steady crack propagation conditions. Such behaviour is attributed to the formation of a crazing zone ahead of the crack tip, which develops prior to crack propagation. Once the steady regime is attained, the crack advances in a self-similar manner. In the proposed creep crack growth rate model, only the steady-state propagation phase is considered.

Similar curves were observed for the other specimens. Fig. 11 plots the da/dt vs G/G_c curves for the RWDC and the TDCB constant load tests, where G/G_c is the normalized energy release rate (Table 3) with the fracture toughness found for each specimen. The RWDC results in Fig. 11 are from Fig. 3 and taken from Ref. [14]. There is some offset between both curves. Although, they are different types of specimens and loaded in a different manner, the coefficient that describes the slope of the power law is similar.

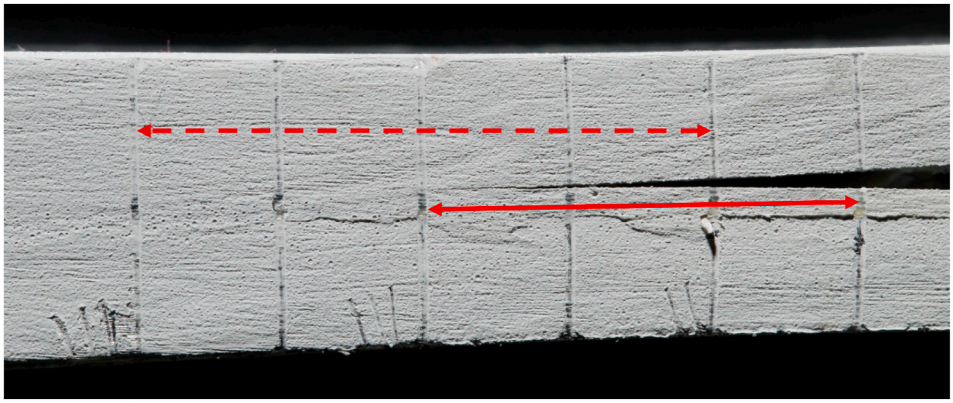

Fig. 7. Example of TDCB specimen with the dashed red arrow indicating the measurement distance for the calibration of the pixels in the photos and the solid red arrow the crack length measurement from the tip of the pre-crack.

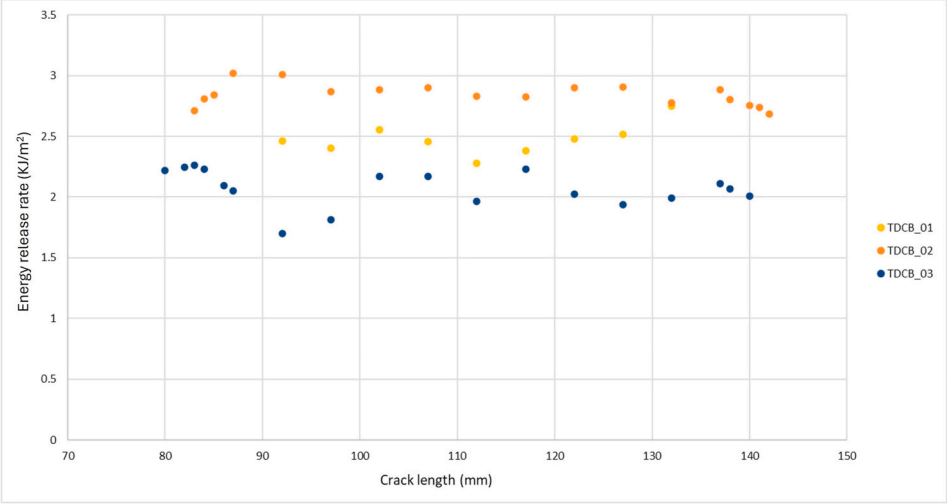

Fig. 8. Energy release rate vs crack length of the three quasi-static TDCB tests. Energy release rate determined with the ECM data reduction method.

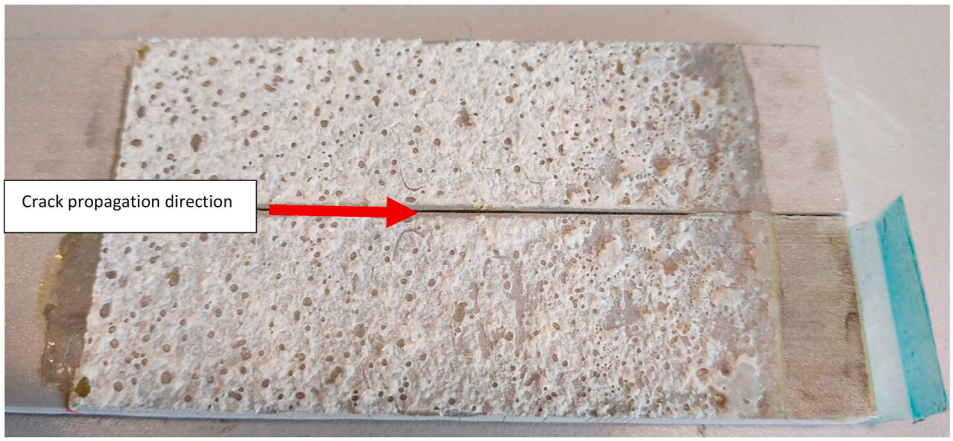

Fig. 9. The cohesive fracture surface of specimen TDCB_01.

Table 2
Overview of the three TDCB specimens that are tested quasi-static.

Specimen	G_c - ECM (KJ/m^2)		dC/da (N^{-1})	B (mm)
	Avg.	Std. Dev.		
TDCB_01	2.488	0.136	0.0013	24.95 ± 0.04
TDCB_02	2.823	0.071	0.0014	24.93 ± 0.02
TDCB_03	2.067	0.094	0.0013	24.84 ± 0.04
Average: (Batch)	2.459			
Std. Dev. (Batch)	0.309			

Table 3
Overview of the four TDCB specimens that are tested with a constant applied load.

Specimen	Load (N)	B (mm)	G - ECM (KJ/m^2)	da/dt (mm/h)
TDCB_CL_01	203	24.90 ± 0.08	1.07	0.315
TDCB_CL_02	222	24.84 ± 0.04	1.29	0.493
TDCB_CL_03	242	24.91 ± 0.04	1.49	1.343
TDCB_CL_04	274	24.93 ± 0.10	1.96	1.714

The fracture surfaces of the four tested specimens are shown in Fig. 12. The pre-crack shows primarily cohesive failure as was observed for the specimens tested quasi-static. Then a transition to adhesive failure is visible. When the specimens fail (the last part of the adhesive), it fractures in an unstable manner, so a much higher crack growth rate. This results in a transition to cohesive failure again. This last part is not considered in the results as presented in Fig. 10. It can also be noticed that, if a higher constant load is applied, the proportion of adhesive failure reduces, and more parts of cohesive failure are visible.

4.3. TDCB numerical model with RWDC data

Four simulations were run with similar loads (Table 4) that were applied in the TDCB constant load tests (Table 3). The resulting crack growth rate is extracted from the numerical model as the time required for one node pair at the surface-to-surface contact to release.

The TDCB FEM results are plotted in Fig. 13 together with the RWDC and TDCB experimental creep crack growth data. The TDCB FEM model follows the RWDC experimental data, as expected, since the CCGM parameters adjusted from the RWDC test results are inserted in the Paris' law-like equation of the DC module.

5. Discussion

Two main results of this work are discussed in this section. Firstly, the TDCB constant load test results compared to the proposed CCGM. Secondly, how the CCGM could be used in existing numerical models and how those results correlate with the experimental work.

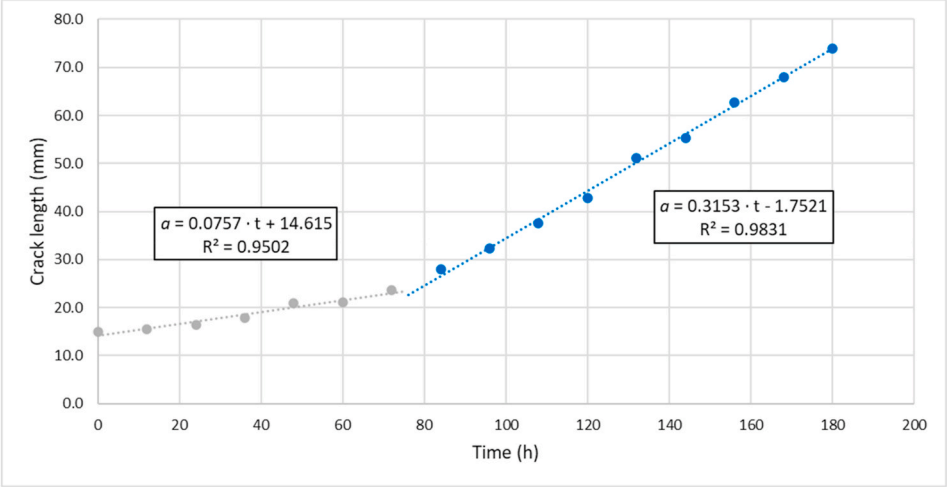

Fig. 10. Crack length (a) measured in the photos taken during the test of TDCB_CL_01 and plotted against time (t) in hours. The slope of the blue trendline is considered to be the propagation slope and provides the average creep crack growth rate.

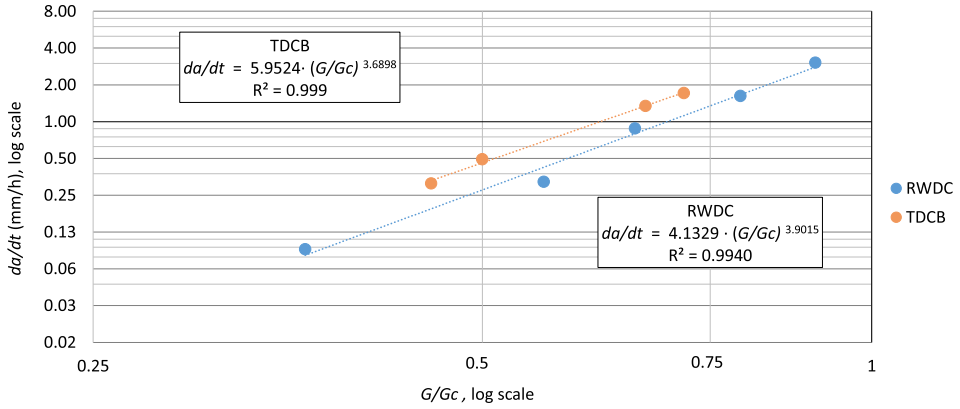

Fig. 11. Crack growth rate (da/dt) against normalized energy release rate (G/G_c) on a log-log scale with the data of the RWDC tests and the results found for the constant load TDCB tests [14].

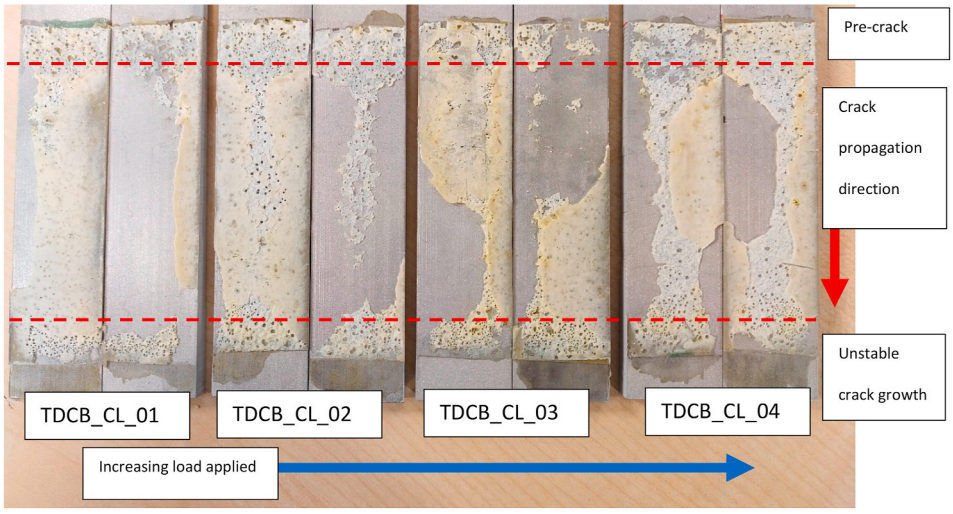

Fig. 12. Fracture surface of the TDCB constant load specimens with from left to right increasing load applied.

Table 4
Overview of the data from the four TDCB FEM simulations.

Specimen	Load (N)	G (KJ/m^2)	da/dt (m/s)
TDCB_FEM_01	200	1.09	$1.40 \bullet 10^{-8}$
TDCB_FEM_02	220	1.31	$2.85 \bullet 10^{-8}$
TDCB_FEM_03	240	1.55	$5.80 \bullet 10^{-8}$
TDCB_FEM_04	270	1.99	$1.54 \bullet 10^{-7}$

5.1. The TDCB as a reference specimen to validate the CCGM

The results of the TDCB constant load tests are used to show that the CCGM also describes the creep crack growth in a bonded joint with the same adhesive but a different geometry. In the quasi-static TDCB test results it can be observed that, once the fracture toughness is reached it remains stable during the rest of the crack propagation phase.

For the RWDC test method, the applied energy release rate is normalized with the average fracture toughness found with the quasi-static RWD test setup [15]. The same principle has been tried for the TDCB constant load test results. Although, it was discovered that there is also spread in the results between the quasi-static TDCB tests and the individual specimens for the TDCB constant load test.

Looking to the different load levels applied and the creep crack growth rates observed for the different specimens (Table 3), a linear trendline on a log-log scale is expected as was found for this adhesive in the RWDC test method. In the case of the TDCB the data can also be normalized which, then produces the graph as shown in Fig. 11, where it can be observed that the slope of the creep crack growth model (CCGM) curve is similar for both the RWDC and TDCB. Although, the parameter c of the CCGM is slightly off and could be caused by the overestimation of the RWDC test method. From previous work it is known that the RWD test method very likely overestimates the fracture toughness due to the friction of the roller wedge [15]. The presented RWDC curve assumes that the friction in the roller wedge can be neglected since it is so low and therefore taken as zero. If the very low friction is taken into account then it is not easy to determine this accurately. In previous work an estimation was made for the magnitude of the friction coefficient of the roller wedge and is likely around 0.02 [15]. In Fig. 14, the RWDC curve is corrected assuming the friction coefficient is 0.02 (RWDC 0.02). The slope of the RWDC gets closer to the slope found with the TDCB but the offset between both curves remains. The cause of this offset between both curves remains ambiguous. Conducting a thorough investigation into the distinct stress fields at the crack tips induced by variations in specimen arm thickness and test configurations could elucidate this issue.

The results show that the TDCB constant load test can produce creep crack growth curves. But the TDCB constant load test method is never considered as a suitable test method for industry for the following reasons. The specific geometry of the TDCB specimens requires the adherends to be manufactured with a milling machine, while the RWDC method requires simpler DCB-like specimens. The adherends for the DCB-like specimens can be easily cut from a plate or strip which is more affordable than milling, and if fibre reinforced plastics are used making a specific TDCB geometry is complex. The constant load that needs to be applied to the specimen in the RWDC test setup to have a similar energy release rate at the crack tip as the TDCB is approximately 19 % of the weight required for the TDCB constant load test, which results in a more practical and safer to use test method. Comparing the RWDC method to the TDCB constant load test, the latter requires crack length measurement during the test, for the RWDC method the crack growth rates follow directly from the wedge displacement measurement. Measuring the wedge displacement with a LVDT is a continuous measurement method that is more accurate and gives more information about how the adhesive behaves over a long time period. To initiate the creep crack growth tests a sharp crack tip must be created, which is done by pre-cracking the specimen. The TDCB specimens require a displacement

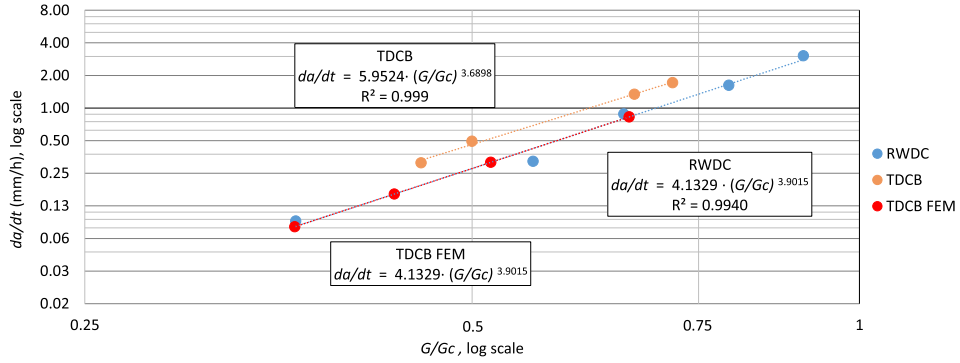

Fig. 13. Creep crack growth rate against normalized energy release rate on a log-log scale with the data of the RWDC tests, constant load TDCB tests and the TDCB FEM model.

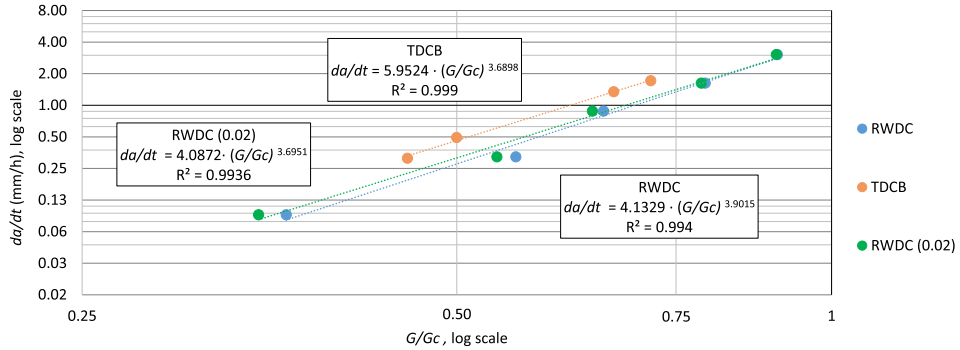

Fig. 14. RWDC curve corrected by assuming a friction coefficient of 0.02 in the roller wedge instead of assuming a friction coefficient of zero.

controlled tensile test machine to pre-crack the specimen before loading it in the TDCB constant load test setup. The RWD test setup can be used with the manual method [15] (pushing the roller wedge in the specimen by turning a threaded bar) to create a pre-crack, which does not require a test machine. In the same test setup then a constant load can be applied to the wedge to immediately start the RWDC test after creating the pre-crack.

5.2. Existing fatigue model to simulate creep crack growth in a bonded joint

Fatigue is a durability phenomenon that is already known for a long time and has been extensively researched for metals and composite materials. Therefore, numerical models have been developed and implemented in commercially available software. For creep crack growth such models are less widely available but the behaviour from the creep crack growth experimental results (Fig. 13) show that it also follows a power law behaviour similar as the Paris' law-like expression for fatigue. Looking at some examples in literature related to fatigue testing or modelling of DCB bonded joints, quite some spread in results of the material parameters can be found. Ranging from 1 to 9 for the power coefficient that determines the slope of the Paris' law-like expression [32–38]. The material parameter found for the slope of the curve for this specific adhesive system is approximately 3.9 (Fig. 3).

The empirical material parameters of the creep crack growth curve of the RWDC test are implemented in the FEM model of the TDCB constant load test. The geometry and the material properties of the TDCB adherends in the model result in an energy release rate at the crack tip for different constant loads applied. The constant load applied relating to the energy release rate at the crack tip (Table 4) matches well with what was analytically determined with the ECM data reduction method for the TDCB experimental tests (Table 3). Even though the FEM model is a TDCB specimen, the crack growth rate obtained from the model matches with the creep crack growth rates found in RWDC test results (Fig. 13). This means that the VCCT and DC module only follow the Paris' law-like expression (empirical material parameters from RWDC test).

6. Conclusions

A Creep Crack Growth Model (CCGM) is proposed to predict creep crack growth based on applied energy release rate. The model parameters are obtained by experimental tests using the RWD creep crack growth (RWDC) test method [14]. It is demonstrated that the CCGM can be implemented into an existing commercially available numerical model. The CCGM and the RWDC method are validated against a TDCB specimen that is loaded with a constant weight.

Results of the creep crack growth rate tests show that, for this specific tested adhesive system, a similar slope is obtained for the CCGM with both the TDCB constant load test and the RWDC test method. Based on these results, it can be assumed that the CCGM describes the creep crack growth rate in the bonded joint. The TDCB constant load test is able to produce creep crack growth results. However, it is not a suitable method for industry to obtain creep crack growth curves. The TDCB constant load test has as practical disadvantages over the RWDC method that it requires visual crack length measurement, a tensile test machine to pre-crack the specimen and the adherends must be milled into a tapered geometry with specific dimensions.

Finite element method (FEM) results of the modelled TDCB specimen demonstrate that existing commercially available fatigue models based on a Paris' law-like expression can be used to simulate creep crack growth in a bonded joint. Entering the experimental material parameters of the CCGM in the direct cyclic (DC) module of the FEM model gives the same results as the RWDC test. This shows that the DC module follows exactly the prescribed CCGM, and that the energy release rate controls the crack growth rate. It must be mentioned that this principle only has been demonstrated for this specific adhesive system and using the DC + VCCT modules in Abaqus. Furthermore, it has only been tested on relatively simple straight bonded joints between two similar material types loaded in mode I.

In conclusion, the durability of bonded joints is a critical aspect of many engineering applications, a better prediction of what creep crack growth rates to expect when a certain energy release rate is present at the crack tip will reduce the uncertainty involved in design of bonded joint for durability. This work presents an overall methodology to measure and simulate creep crack growth in bonded joints, which is validated with TDCB tests.

CRediT authorship contribution statement

E. Meulman: Conceptualization, Data curation, Formal analysis, Investigation, Methodology, Validation, Writing – original draft, Writing – review & editing. **J. Renart:** Conceptualization, Formal analysis, Funding acquisition, Supervision, Writing – review & editing, Validation. **L. Carreras:** Conceptualization, Formal analysis, Supervision, Validation, Writing – review & editing. **J. Zurbitu:** Conceptualization, Formal analysis, Supervision, Validation, Writing – review & editing.

Declaration of competing interest

The authors declare the following financial interests/personal relationships which may be considered as potential competing interests: Jordi Renart has patent #Patent number: 300352094, PCT/ES2020/070074 issued to -. If there are other authors, they declare that they have no known competing financial interests or personal relationships that could have appeared to influence the work reported in this paper.

Data availability

Data will be made available on request.

Acknowledgements

The work was performed under contract PID2021-127879OB-C21 of the Spanish Government through the Ministerio de Ciencia, Innovación y Universidades. The authors would like to acknowledge the support for this work by these entities. E. M. received additional support through a fellowship grant, IFUdG2021-AE, co-funded by the AMADE research group (GRCT0064) and provided by the Universitat de Girona and Banco Santander. L.C. acknowledges the grant RYC2021-032171-I funded by MCIN/AEI/10.13039/501100011033 and by "European Union NextGenerationEU/PRTR. Open Access funding provided thanks to the CRUE-CSIC agreement with Elsevier. The work in this research has been made possible by patent 300352094, PCT/ES2020/070074 made available by IKERLAN, S.COOP. (IKER018) and the Universitat de Girona. Furthermore, the authors like to acknowledge the support from the AMADE research group testing laboratory. Author J. Renart is a Serra Húnter fellow. Open Access funding was provided thanks to the CRUE-CSIC agreement with Elsevier.

References

[1] Da Silva LFM, Öchsner A, Adams RD. Handbook of adhesion technology. second ed. Springer International Publishing AG; 2011. https://doi.org/10.1007/978-3-642-01169-6.
[2] Bradley W, Cantwell WJ, Kausch HH. Viscoelastic creep crack growth: a review of fracture mechanical analyses. Mech Time-Dependent Mater 1997;1(3):241–68. https://doi.org/10.1023/A:1009766516429.
[3] Siviour CR, Jordan JL. High strain rate Mechanics of polymers: a review. J Dyn Behav Mater Mar. 2016;2(1):15–32. https://doi.org/10.1007/s40870-016-0052-8.
[4] Cavezza F, Boehm M, Terryn H, Hauffman T. A review on adhesively bonded aluminium joints in the automotive industry. Metals (Basel) 2020;10(6):1–32. https://doi.org/10.3390/met10060730.
[5] Broughton WJ, Mera RD. May. Review of durability test methods and standards for assessing long term performance of adhesive joints. 1997. p. 78 [Online].

Available: http://www.adhesivestoolkit.com/Docu-Data/NPLDocuments/PAJ/PAJReports/PAJ3Reports/PAJ3Report1CMMT(A)61.pdf. [Accessed 9 March 2023].
[6] ASTM D3762-03(2010) standard test method for adhesive-bonded surface durability of aluminum (wedge test) (withdrawn 2019). ASTM International; 2010. p. 5 [Online]. Available: https://www.astm.org/Standards/D3762.htm.
[7] Adams DO, DeVries KL, Child C. Durability of adhesively bonded joints for aircraft structures. In: FAA Joint Adv Materials and Structures (JAMS) Center of Excellence Technical Review Meeting; 2012. p. 22 [Online]. Available: http://depts.washington.edu/amtas/events/jams_12/papers/paper-adams_adhesive.pdf.
[8] Cognard J. Use of the wedge test to estimate the lifetime of an adhesive joint in an aggressive environment. Int J Adhesion Adhes 1986;6(4):215–20. https://doi.org/10.1016/0143-7496(86)90008-4.
[9] Plausinis D, Spelt JK. Application of a new constant G load-jig to creep crack growth in adhesive joints. Int J Adhesion Adhes 1995;15(4):225–32. https://doi.org/10.1016/0143-7496(96)83703-1.
[10] Dillard DA, Wang JZ, Parvatareddy H. A simple constant strain energy release rate loading method for double cantilever beam specimens. J Adhes Jun. 1993;41(1–4):35–50. https://doi.org/10.1080/00218469308026553.
[11] Lefebvre DR, Dillard DA, Brinson HF. The development of a modified double-cantilever-beam specimen for measuring the fracture energy of rubber to metal bonds. Exp Mech Mar. 1988;28(1):38–44. https://doi.org/10.1007/BF02328994.
[12] Nakamura K, Sekiguchi Y, Shimamoto K, Houjou K, Akiyama H, Sato C. Creep crack growth behavior during hot water immersion of an epoxy adhesive using a spring-loaded double cantilever beam test method. Materials Jan. 2023;16(2). https://doi.org/10.3390/ma16020607.
[13] Schrader P, Schmandt C, Marzi S. Mode I creep fracture of rubber-like adhesive joints at constant crack driving force. Int J Adhesion Adhes 2022;113(Mar). https://doi.org/10.1016/j.ijadhadh.2021.103079.
[14] Meulman E, Renart J, Carreras L, Zurbitu J. A methodology for the experimental characterization of energy release rate-controlled creep crack growth under mode I loading. Eng Fract Mech Apr. 2023;283:109222. https://doi.org/10.1016/j.engfracmech.2023.109222.
[15] Meulman E, Renart J, Carreras L, Zurbitu J. Analysis of mode I fracture toughness of adhesively bonded joints by a low friction roller wedge driven quasi-static test. Eng Fract Mech May 2022;271:108619. https://doi.org/10.1016/j.engfracmech.2022.108619.
[16] Manterola J, Renart J, Zurbitu J, Turon A, Urresti I. Mode I fracture characterization of rigid and flexible bonded joints using an advanced Wedge Driven Test. Mech Mater 2020;148(103534):13. https://doi.org/10.1016/j.mechmat.2020.103534.
[17] Renart J, Costa J, Santacruz G, Lazcano S, Gonzalez E. Measuring fracture energy of interfaces under mode I loading with the wedge driven test. Eng Fract Mech 2020;239:15. https://doi.org/10.1016/j.engfracmech.2020.107210.
[18] ISO 25217:2009 - Adhesives — determination of the mode 1 adhesive fracture energy of structural adhesive joints using double cantilever beam and tapered double cantilever beam specimens. 2009. p. 24.
[19] Blackman BRK, Hadavinia H, Kinloch AJ, Paraschi M, Williams JG. The calculation of adhesive fracture energies in mode I: revisiting the tapered double cantilever beam (TDCB) test. Eng Fract Mech Jan. 2003;70(2):233–48. https://doi.org/10.1016/S0013-7944(02)00031-0.
[20] Blackman BRK, Kinloch AJ, Paraschi M, Teo WS. Measuring the mode I adhesive fracture energy, GIc, of structural adhesive joints: the results of an international round-robin. Int J Adhesion Adhes 2003;23(4):293–305. https://doi.org/10.1016/S0143-7496(03)00047-2.
[21] Blackman BRK, Kinloch AJ, Rodriguez Sanchez FS, Teo WS, Williams JG. The fracture behaviour of structural adhesives under high rates of testing. Eng Fract Mech Dec. 2009;76(18):2868–89. https://doi.org/10.1016/j.engfracmech.2009.07.013.
[22] Hesebeck O, Meyer U, Sondag A, Brede M. Investigations on the energy balance in TDCB tests. Int J Adhesion Adhes Jun. 2016;67:94–102. https://doi.org/10.1016/j.ijadhadh.2015.12.031.
[23] Qiao P, Wang J, Davalos JF. Tapered beam on elastic foundation model for compliance rate change of TDCB specimen. Eng Fract Mech Jan. 2003;70(2):339–53. https://doi.org/10.1016/S0013-7944(02)00023-1.
[24] Tsang WL. The use of tapered double cantilever beam (TDCB) in investigating fracture properties of particles modified epoxy. SN Appl Sci Apr. 2020;2(4). https://doi.org/10.1007/s42452-020-2487-8.
[25] Teixeira JMD, Campilho RDSG, da Silva FJG. Numerical assessment of the double-cantilever beam and tapered double-cantilever beam tests for the GIC determination of adhesive layers. J Adhes Sep. 2018;94(11):951–73. https://doi.org/10.1080/00218464.2017.1383905.
[26] Marzi S, Biel A, Stigh U. On experimental methods to investigate the effect of layer thickness on the fracture behavior of adhesively bonded joints. Int J Adhesion Adhes Dec. 2011;31(8):840–50. https://doi.org/10.1016/j.ijadhadh.2011.08.004.
[27] Abaqus analysis user's manual. Dassault Systemes Simulia, Inc; 2014.
[28] Pirondi A, Giuliese G, Moroni F, Bernasconi A, Jamil A. Comparative study of cohesive zone and virtual crack closure techniques for three-dimensional fatigue debonding. J Adhes Jun. 2014;90(5–6):457–81. https://doi.org/10.1080/00218464.2013.859616.
[29] Dávila CG, Bisagni C. Fatigue life and damage tolerance of postbuckled composite stiffened structures with initial delamination. Compos Struct Feb. 2017;161:73–84. https://doi.org/10.1016/j.compstruct.2016.11.033.
[30] Teimouri F, Heidari-Rarani M, Haji Aboutalebi F. An XFEM-VCCT coupled approach for modeling mode I fatigue delamination in composite laminates under high cycle loading. Eng Fract Mech May 2021;249:107760. https://doi.org/10.1016/j.engfracmech.2021.107760.
[31] Williams JG. End corrections for orthotropic DCB specimens. Compos Sci Technol 1989;35(4):367–76. https://doi.org/10.1016/0266-3538(89)90058-4.
[32] Ashcroft IA, Shaw SJ. Mode I fracture of epoxy bonded composite joints 2. Fatigue loading. Int J Adhesion Adhes Jan. 2002;22(2):151–67. https://doi.org/10.1016/S0143-7496(01)00050-1.
[33] Fernández MV, de Moura MFSF, da Silva LFM, Marques AT. Composite bonded joints under mode I fatigue loading. Int J Adhesion Adhes 2011;31(5):280–5. https://doi.org/10.1016/j.ijadhadh.2010.10.003.
[34] Pirondi A, Nicoletto G. Fatigue crack growth in bonded DCB specimens. Eng Fract Mech 2004;71(4–6):859–71. https://doi.org/10.1016/S0013-7944(03)00046-8.
[35] de Moura MFSF, Gonçalves JPM, Fernandez MV. Fatigue/fracture characterization of composite bonded joints under mode I, mode II and mixed-mode I+II. Compos Struct Apr. 2016;139:62–7. https://doi.org/10.1016/j.compstruct.2015.11.073.
[36] Ishii K. Effect of substrate material on fatigue crack propagation rate of adhesively bonded DCB joints. J Adhes Sci Technol 2012;25(20):2775–87. https://doi.org/10.1163/016942410X537369.
[37] Campos AAMA, De Jesus AMP, Correia JAFO, Morais JJL. Fatigue crack growth behavior of bonded aluminum joints. In: Procedia engineering. Elsevier Ltd; 2016. p. 270–7. https://doi.org/10.1016/j.proeng.2016.08.890.
[38] Carreras L, Renart J, Turon A, Costa J, Essa Y, Martin de la Escalera F. An efficient methodology for the experimental characterization of mode II delamination growth under fatigue loading. Int J Fatig 2017;95:185–93. https://doi.org/10.1016/j.ijfatigue.2016.10.017.